"Resistance Is Futile": Weaker Selection for Resistance by Abundant Parasites Increases Prevalence and Depresses Host Density

Jason C. Walsman,[1,*] Meghan A. Duffy,[2] Carla E. Cáceres,[3] and Spencer R. Hall[4]

1. University of Pittsburgh, Pittsburgh, Pennsylvania 15260; 2. University of Michigan, Ann Arbor, Michigan 48109; 3. University of Illinois at Urbana-Champaign, Champaign, Illinois 61820; 4. Indiana University, Bloomington, Indiana 47405

Submitted May 28, 2022; Accepted November 23, 2022; Electronically published April 25, 2023

Online enhancements: supplemental PDF.

ABSTRACT: Theory often predicts that host populations should evolve greater resistance when parasites become abundant. Furthermore, that evolutionary response could ameliorate declines in host populations during epidemics. Here, we argue for an update: when all host genotypes become sufficiently infected, higher parasite abundance can select for lower resistance because its cost exceeds its benefit. We illustrate such a "resistance is futile" outcome with mathematical and empirical approaches. First, we analyzed an eco-evolutionary model of parasites, hosts, and hosts' resources. We determined eco-evolutionary outcomes for prevalence, host density, and resistance (mathematically, "transmission rate") along ecological and trait gradients that alter parasite abundance. With high enough parasite abundance, hosts evolve lower resistance, amplifying infection prevalence and decreasing host density. In support of these results, a higher supply of nutrients drove larger epidemics of survival-reducing fungal parasites in a mesocosm experiment. In two-genotype treatments, zooplankton hosts evolved less resistance under high-nutrient conditions than under low-nutrient conditions. Less resistance, in turn, was associated with higher infection prevalence and lower host density. Finally, in an analysis of naturally occurring epidemics, we found a broad, bimodal distribution of epidemic sizes consistent with the resistance is futile prediction of the eco-evolutionary model. Together, the model and experiment, supplemented by the field pattern, support predictions that drivers of high parasite abundance can lead to the evolution of lower resistance. Hence, under certain conditions, the most fit strategy for individual hosts exacerbates prevalence and depresses host populations.

Keywords: host evolution, infectious disease, eco-evolutionary feedbacks, experimental evolution.

Introduction

Infectious diseases threaten many populations (Dobson et al. 2008), posing risks to livestock (Horan and Fenichel 2007) and species of conservation concern, such as birds and amphibians (Cooper et al. 2009; Vredenburg et al. 2010). Parasites harm their hosts by decreasing survival ("mortality virulence") or decreasing birth rate ("fecundity reduction or castration"; Ebert et al. 2000). Such virulence can reduce host density and increase extinction risk (Ebert et al. 2000). However, in the face of selective pressure and given sufficient genetic variance, hosts can evolve resistance to infection (via prevention of infection) in populations experiencing outbreaks. This evolution of resistance during the epidemic should reduce infection prevalence (proportion of hosts infected) and ameliorate depression of host density (Altizer et al. 2003; Duffy and Sivars-Becker 2007; Christie and Searle 2018), perhaps rapidly (Penczykowski et al. 2011). Such rapid evolution of resistance might even help terminate epidemics (Duffy and Sivars-Becker 2007; Duffy et al. 2009).

However, such evolution of resistance can hinge on its cost. Resistance becomes costly when linked to fecundity or other traits (Boots and Begon 1993; Hall et al. 2010; Duncan et al. 2011; van der Most et al. 2011; Auld et al. 2013). Hence, host populations without parasites should evolve decreased resistance (given its cost without benefit), as seen in, for example, poultry (van der Most et al. 2011), wildflowers (O'Hara et al. 2016), paramecia (Duncan et al. 2011), and nematodes (via evolution of selfing; Slowinski et al. 2016). With parasites, the cost of resistance may become worth paying, depending on its benefit (preventing infection and virulence). This benefit depends on the abundance of parasites and the force of infection. For example, when ecological drivers make parasites scarce and epidemics small (Duffy et al. 2012), hosts can evolve less resistance. Then, as ecological drivers increase parasite abundance, hosts typically evolve more resistance (Frank

* Corresponding author; email: walsmanjason@gmail.com.

American Naturalist, volume 201, number 6, June 2023. https://doi.org/10.1086/724426

1994; Boots et al. 2009; Duffy and Forde 2009; Duffy et al. 2012; Lopez-Pascua et al. 2014; Koskella 2018). This prediction holds especially strongly for parasites that completely castrate (Bohannan and Lenski 1997, 2000; Boots and Haraguchi 1999; Lopez-Pascua et al. 2014; Gomez et al. 2015). Thus, theory typically predicts that hosts should evolve resistance when ecological factors drive increased parasite abundance because the benefit of resistance exceeds the cost.

This evolutionary response can flip if infected hosts can reproduce. In fact, high enough parasite abundance can select for lower resistance (Bonds et al. 2005; Miller et al. 2007; Donnelly et al. 2015; Best et al. 2017). Hence, the fittest strategy for costly resistance becomes a hump-shaped function of the drivers of higher parasite abundance (Donnelly et al. 2015). At low parasite abundance, resistance offers little benefit, as all genotypes experience similar low rates of infection. But intermediate parasite abundance selects for resistance, as more resistant genotypes benefit from less infection (Donnelly et al. 2015). Yet at even higher parasite abundance, lower resistance can become most fit again. This outcome arises once all genotypes face similarly high probabilities of infection. Then the benefit of resistance contributes little to relative fitness (Donnelly et al. 2015). Instead, the fecundity cost of resistance reigns supreme. Hence, when drivers lead to very high parasite abundance, "resistance is futile."

Here, we illustrate conditions and consequences for resistance is futile evolution with math and data. We first develop it with focus on a driver that we can manipulate (carrying capacity of hosts' resources). We then show its population-level consequences for infection prevalence and host density (unlike most previous work; for a partial exception, see Miller et al. 2007). While decreased resistance increases prevalence, the density response is more complex. Generally, adaptive evolution may increase or decrease host density, most dramatically in evolutionary rescue (increase; Carlson et al. 2014) or suicide (decrease; Rankin and López-Sepulcre 2005). In the present problem, the impact of resistance on host density depends on parasite abundance, the cost of resistance, and the responses of other populations (e.g., resources) to host traits. As a result, host density may increase or decrease with resistance. We show how resistance evolution, given its ecological context, affects host density using nonevolving, ecology-only populations. We also evaluate evolution as competition between two host genotypes at equilibrium or during transient epidemics. All of these modeling perspectives point to the same conclusion: as ecological drivers lead to high parasite abundance, the resistance is futile mechanism can amplify prevalence and depress host density.

We then test these predictions qualitatively with a mesocosm experiment in a planktonic system. In this system, infection with a fungal parasite (*Metschnikowia bicuspidata*) increases the mortality of infected zooplankton hosts (*Daphnia dentifera*). However, infected hosts can still reproduce. Additionally, hosts face a fecundity-resistance trade-off (via a foraging rate mechanism; Hall et al. 2010; Auld et al. 2013). Both features meet model assumptions. In mesocosms, we manipulated the carrying capacity of hosts' resources, and higher nutrient supply supported denser host populations and larger epidemics. All populations started with the same mean level of resistance. After clonal turnover, high-nutrient (high-parasite) populations became less resistant than low-nutrient (low-parasite) populations. Across these high-nutrient populations, lower resistance correlated with higher prevalence and lower host density. Finally, we looked to a survey of epidemics in lake populations of the focal fungus in its plankton host for concordant results. We found a somewhat bimodal, right-skewed, widely spread distribution of epidemics. While providing only indirect evidence, this field distribution was consistent with the resistance is futile mechanism. Hence, the models and experiment support a resistance is futile effect that may help explain distributions of epidemics in the field.

Eco-Evolutionary Model of Resources, Hosts, and Parasites

The Model

The resistance is futile prediction arises in an eco-evolutionary model analyzed under equilibrium and non-equilibrium conditions. Inspired by the planktonic system, this model allows for full feedbacks of resources (R), susceptible (S_i) and infected (I_i) hosts of genotype i, and free-living parasite propagules (Z). We use reasonable parameters values for the focal planktonic system (see table 1; Hall et al. 2010; Strauss et al. 2015; Strauss et al. 2019):

$$\frac{dR}{dt} = wR\left(1 - \frac{R}{K}\right) - f_{\text{av}}R(S_{\text{T}} + I_{\text{T}}), \tag{1a}$$

$$\frac{dS_i}{dt} = ef_iR(S_i + \theta I_i) - \delta S_i - \beta_i S_i Z, \tag{1b}$$

$$\frac{dI_i}{dt} = \beta_i S_i Z - (\delta + \nu)I_i, \tag{1c}$$

$$\frac{dZ}{dt} = \sigma(\delta + \nu)I_{\text{T}} - mZ. \tag{1d}$$

Resources grow logistically with intrinsic rate of increase w and carrying capacity K (first term, eq. [1a]). They are consumed by the sum of susceptible and infected hosts ($H = S + I$) of genotypes $i = 1$ to n ($S_{\text{T}} = \sum_{i=1}^{n} S_i$,

Table 1: Symbols, meaning, and default values or ranges for state variables, functions of state variables, and traits and other parameters in an eco-evolutionary model of hosts, parasites, and resources (eqq. [1])

Symbol	Meaning	Unit	Value or range
State variables:			
t	Time	day	Varies
R	Density of resources	μg chl a L^{-1}	See figures
S_i	Density of susceptible host i	hosts L^{-1}	See figures
I_i	Density of infected host i	hosts L^{-1}	See figures
Z	Density of parasite propagules	parasites L^{-1}	Varies
Functions:			
H	Total density of hosts, $S + I$	hosts L^{-1}	See figures
p	Prevalence, I/H	unitless	See figures
Traits and other parameters:			
f_{max}	Maximum foraging rate (eq. [2])	L host^{-1} day^{-1}	.0207[a]
f_{min}	Minimum foraging rate (eq. [2])	L host^{-1} day^{-1}	.0052[a]
f_{scale}	Trade-off parameter (eq. [2])	parasites host^{-1}	2,984[a]
e	Conversion efficiency	hosts μg chl a^{-1}	.18[b]
f_i	Foraging rate, host i	L host^{-1} day^{-1}	f_{min} to f_{max}
K	Carrying capacity, resource	μg chl a L^{-1}	30, 25 to 150[b]
m	Loss rate of parasites	day^{-1}	1.5[c]
v	Mortality virulence	day^{-1}	.05[b]
w	Intrinsic rate of increase, R	day^{-1}	.9[b]
δ	Background mortality rate	day^{-1}	.05[b]
β_i	Transmission rate from propagules to host i	L parasite^{-1} day^{-1}	0 to 40 × 10^{-6}[d]
θ	Fecundity of infected relative to susceptible hosts	unitless	.65,[e] 0 (castration) to 1 (full fecundity)
σ	Parasites released per host	parasites host^{-1}	100,000[b]

Note: Only traits f_i and β_i vary with host genotype; others are held constant. chl a = chlorophyll a (a measurement of algal biomass).

[a] Trade-off parameters were chosen to match focal clones and give reasonable evolution.

[b] Biologically reasonable values of traits (Strauss et al. 2015).

[c] $m = 1.5$ corresponds to 22% ($e^{-1.5\times1}$) of propagules alive after 1 day. Other values (e.g., Strauss et al. 2015) produce excessively high infection prevalence here.

[d] Biologically reasonable during an epidemic (Strauss et al. 2019).

[e] Biologically reasonable (Hall et al. 2010).

$I_T = \sum_{i=1}^{n} I_i$) foraging at weighted average rate f_{av} ($f_{av} = \sum_{i=1}^{n}(f_i H_i / H_T)$).

Each host genotype i differs in two key traits, transmission rate and foraging rate. More specifically, these fixed traits are (1) the per-parasite, per-host transmission rate of infection from the environment to hosts β_i and (2) the per-host, per-resource rate of resource capture (i.e., foraging rate f_i). Here, a lower transmission rate provides an "avoidance" form of resistance that prevents infection (Boots and Bowers 1999). Through foraging, hosts also compete for their shared resources (R). Both host classes, S_i and I_i, may convert these resources into susceptible offspring (i.e., transmission is purely horizontal; first term, eq. [1b]). Susceptible hosts do so with a conversion efficiency e. Meanwhile, infected hosts do so with modified efficiency $e\theta$, where $\theta = 1$ means full fecundity while $\theta = 0$ represents complete castration (no production of offspring). Genotypes with a higher foraging rate (e.g., $f_2 > f_1$) have higher fecundity ($ef_2R > ef_1R$ if uninfected and $ef_2R\theta > ef_1R\theta$ if infected), all else equal. We parametrized the model with moderate fecundity reduction for infected hosts (0.65; Hall et al. 2010) but consider a full range of $\theta = 0$–1 (fig. S1). All genotypes experience an identical background mortality rate δ.

Additionally, susceptible hosts become infected at rate β_i by encountering parasite propagules while foraging. Hence, a genotype's foraging rate (f_i) connects to transmission rate by a trade-off (eq. [2]),

$$\beta_i = \frac{f_i}{f_{scale}} \ln\left(\frac{f_{max} - f_{min}}{f_{max} - f_i}\right), \quad (2)$$

as governed by three positive shape parameters (f_{max}, f_{min}, and f_{scale}) and where ln(…) is the natural logarithm. Hence, foraging rate f_i remains bounded, ranging from f_{min} (corresponding to $\beta_i = 0$) to f_{max} (corresponding to $\beta_i = \infty$, ensuring that hosts evolve to less than f_{max}) as scaled by

a constant (f_{scale}). This trade-off has two key features. First, it links three host traits: higher foraging rate (f_i) is associated with higher per capita fecundity (ef_iR or $ef_iR\theta$, at a given R) and increased transmission rate β_i (i.e., decreased resistance). Second, this trade-off shape imposes accelerating costs: increased resistance (decreased β_i) corresponds to a small cost (decreased f_i) when resistance is low (high β_i). But when resistance is high (low β_i), even further investment in resistance imposes very costly foraging reduction. When are accelerating costs justified? This curvature can arise if both exposure and susceptibility (probability of infection once exposed) increase with foraging rate (for suggestive evidence of such a link in this system, see Strauss et al. 2019). Hence, β_i, the product of exposure and susceptibility, increases faster than linearly with f_i. More importantly, accelerating costs offer an important intellectual attribute here. Generally, decelerating costs tend to select for extremely low or extremely high resistance (Boots and Haraguchi 1999). Instead, here the conservative shape we implemented prevents extreme evolution and promotes the existence of a continuously stable strategy (CSS; for proof in the case of $\theta = 0$ that a positive trade-off curvature is necessary, see the supplemental PDF, sec. 1; generally decelerating costs tend to select for extreme traits; Boots and Haraguchi 1999). Hence, this accelerating-cost shape prevents a resistance is futile effect from running wild, selecting for a higher transmission and foraging rate to biologically unrealistic extremes (for a more extreme example of the resistance is futile effect with a less conservative shape, see fig. S2). Yet despite our focal trade-off's conservativeness (eq. [2]), hosts can still evolve extremely high or low transmission rates in the model (fig. 1).

Infection converts susceptible hosts into infected hosts (first term, eq. [1c]). These hosts suffer an elevated death rate due to mortality virulence of infection, $\delta + \nu$ (where ν is the added mortality, assumed equal for all genotypes). When infected hosts die, all genotypes release σ parasite propagules, Z, back into the environment (first term, eq. [1d]). Losses of parasite propagules occur at background rate m.

Overview of Analyses of the Model: Adaptive Dynamics, Two-Clone Equilibria, and Simulations

We captured results of selection on host resistance with three complementary modeling approaches. First, we modeled continuous trait evolution (via adaptive dynamics with stable equilibria; see the supplemental PDF, sec. 1) to any point along the trade-off, assuming that ecological processes happen much faster than evolutionary processes and mutations have a small effect. We show how these outcomes depend on the fecundity of infected hosts with more classical results when infected hosts cannot reproduce. This approach has the advantage of finding where hosts evolve along the entire trade-off. However, it is not fully comparable to experiments in which host genotypes have significantly different traits. Second, we modeled outcomes of competition at stable equilibrium between two host clones with significantly different traits (but still falling along the trade-off; for trait values, see fig. S2*A*). We chose transmission rates for the less resistant ($\beta_2 = 2.48 \times 10^{-6}$, $f_2 = 0.012$) and more resistant ($\beta_1 = 7.22 \times 10^{-7}$, $f_1 = 0.009$) genotypes from a previously measured range (Strauss et al. 2015). Furthermore, we used foraging rates typical of these genotypes during epidemics (Strauss et al. 2019).

Third, still using two genotypes, we relaxed equilibrial assumptions to resemble epidemics in mesocosms more closely. To mimic experimental conditions, we started host densities at 10 hosts L^{-1} (either 100% or a 50:50 mixture of two genotypes) and parasites at 3,600 spores L^{-1}, with resources at their carrying capacity: $S_{\text{initial}} = 10$, $I_{\text{initial}} = 0$, $Z_{\text{initial}} = 3{,}600$, and $R_{\text{initial}} = K$. We simulated (method: Dormand-Prince 4(5), local order 7) eco-evo-epidemics for 150 days to approximate the amount of clonal turnover in the experiment and averaged results from days 100 to 150 (Soetaert et al. 2010). Over time, these simulations approached a stable equilibrium (fig. S3); thus, the choice of 100–150 days parallels averaging over the later portion of the experimental time series (as we implement for our experiment below). The transient average approaches the equilibrium if the averaging window is set later or as initial values start closer to the equilibrium. Nonetheless, these simulations provide a qualitative but direct comparison to the mesocosm experiment while confirming that core patterns of the resistance is futile mechanism still emerge some distance from equilibrium. Indeed, the central findings emerge harmoniously from all three modeling approaches, indicating a stronger level of robustness than if they emerged only from one.

For continuous trait evolution, we use adaptive dynamics (Eshel 1983) to find a CSS for resistance (β_{CSS}). Evolution to such a trait value depends on host invasion fitness, which we find as the lifetime reproductive output (R_0, not to be confused with R for resources) of an individual of a mutant genotype (m) when rare and invading the environment created by the resident (r):

$$R_0 \text{ of } m \text{ when invading } r = \underbrace{\frac{ef_m R_r^*}{\delta + \beta_m Z_r^*}}_{\substack{\text{output while} \\ \text{susceptible}}} + \underbrace{\frac{\beta_m Z_r^*}{\delta + \beta_m Z_r^*}}_{\substack{\text{probability of} \\ \text{infection}}} \times \underbrace{\frac{ef_m R_r^* \theta}{\delta + \nu}}_{\substack{\text{output while} \\ \text{infected}}}, \tag{3}$$

where R_r^* and Z_r^* are the resource and parasite densities, respectively, at the resident's stable equilibrium. The

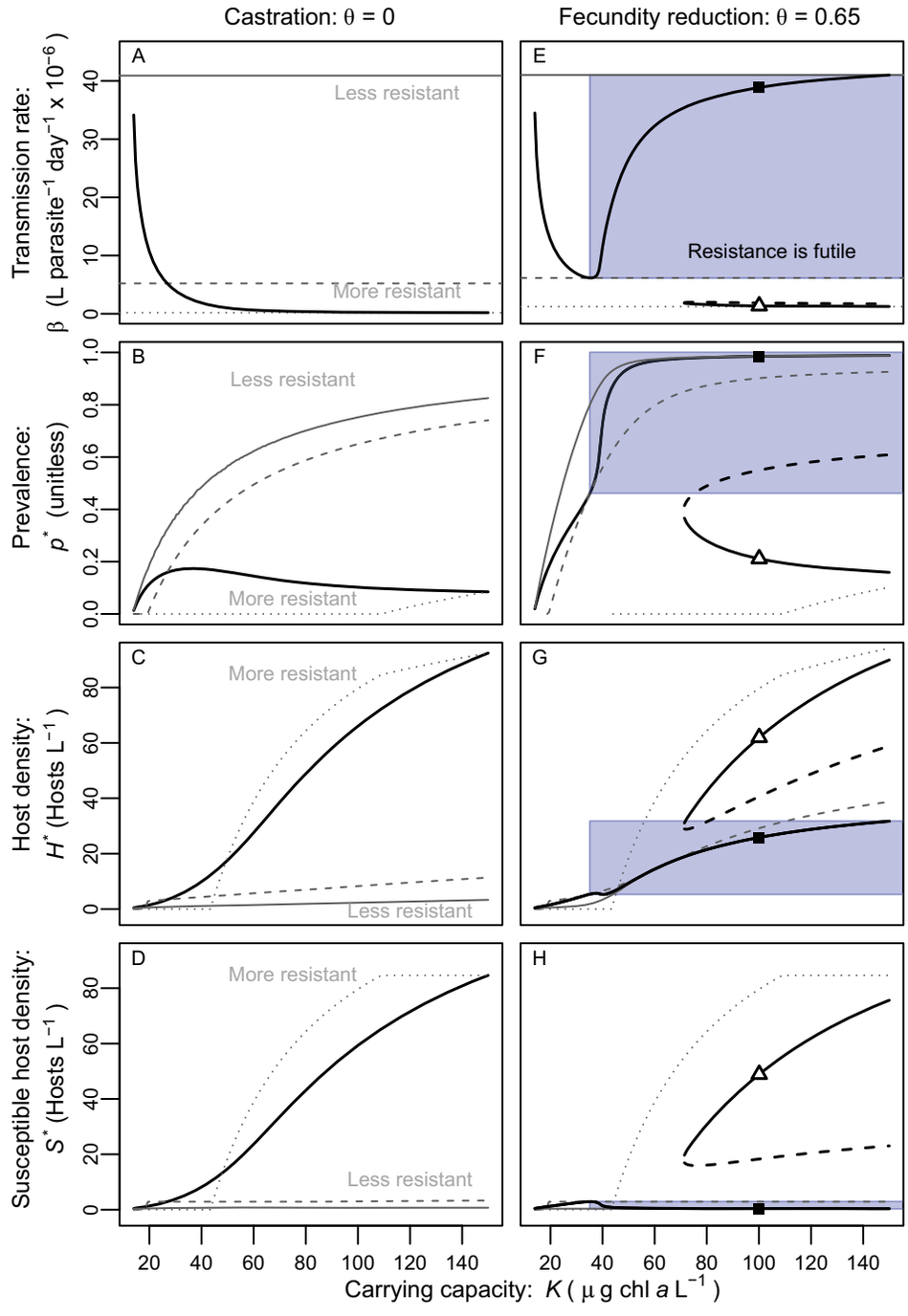

Figure 1: Higher carrying capacity and parasite prevalence can cause hosts to evolve less resistance. Solid black curves represent eco-evolutionary outcomes for transmission rate (β_{CSS}; inverse of resistance) across a gradient of carrying capacity (K). Gray curves denote response of single-reference genotypes (ecology-only populations: solid line = less resistant [high β]; dashed line = medium resistance [medium β]: dotted line = more resistant [low β]). *A–D*, Castration ($\theta = 0$). Hosts evolve increasing resistance (decreasing β_{CSS}) with K (*A*), which keeps prevalence, p^*_{CSS}, much lower relative to ecology-only cases (as p^*_{eco} increases with K; *B*). Higher resistance and lower p^*_{CSS} allow the density of total hosts, H^*_{CSS} (*C*), and susceptible hosts, S^*_{CSS} (*D*), to increase with K. *E–G*, Fecundity reduction ($\theta = 0.65$). Higher resistance first evolves with K, then lower resistance evolves (in the resistance is futile blue box; *E*). At high K, there are two continuously stable strategies (CSSs) separated by a repeller (dashed curve). The black square marks the high β_{CSS} and its associated curves, while the white triangle marks the low β_{CSS}. Prevalence increases with K, more slowly at first, then more quickly as hosts evolve decreasing resistance (blue box; *F*). Total (*G*) and especially susceptible (*H*) host density remain low with K because of low resistance. Note that the solid gray curves fall almost entirely under the solid black curves in *G* and *H*. See table 1 for default parameter values.

reproductive output while susceptible is the fecundity ($ef_mR_r^*$) multiplied by the average duration in the susceptible class ($1/(\delta + \beta_m Z_r^*)$). Infected hosts also contribute to reproduction (at rate $ef_mR_r^*\theta$) while they remain infected ($1/(\delta + \nu)$), but their contribution is scaled by the probability of infection (i.e., the ratio of the flow from S to I divided by all flow from S). If and only if R_0 exceeds 1 can the mutant invade the resident's equilibrium. This same expression for R_0 (eq. [3]) can be found with the next-generation matrix (Hurford et al. 2009). We use adaptive dynamics (Eshel 1983) to find β_{CSS} (which has a corresponding f_{CSS}); when considering trait values near β_{CSS}, the CSS is uninvadable and host populations will evolve toward it (for additional descriptions of a CSS, see the supplemental PDF, sec. 1).

In all three modeling approaches, we varied carrying capacity of the resource (K) as the key ecological driver of parasite abundance. We chose K because we manipulated it in mesocosms (below) by varying nutrient supply and because we described gradients of nutrient supply that increase epidemic size in nature. For a given value of K, we compute host evolution (either β_{CSS} or the frequencies of the two clones) and the corresponding infection prevalence (proportion of hosts infected) and host density. While disease outbreaks may not reach a stable equilibrium, we used long-term attractors (stable equilibria and averages over transient dynamics) to make qualitative predictions. We also calculated outcomes for evolving populations and compared them with those for nonevolving populations along a gradient of resource carrying capacity.

Results: Continuous Trait Evolution

When parasites castrate their hosts ($\theta = 0$), higher carrying capacity (K) leads to the evolution of stronger resistance (lower β_{CSS}). Higher K ecologically increases the density of parasite propagules (Z, not shown) when hosts cannot evolve (i.e., fixed β as gray lines in fig. 1*A*); note that infected host and parasite propagule (Z) densities are proportional at equilibrium (since $Z^* = I^*\sigma(\delta + \nu)/m$ from eq. [1d]). Hence, higher K increases prevalence (p^*; gray curves in fig. 1*B*). In response, host populations evolve increasing resistance (black curve in fig. 1*A*), and prevalence (p_{CSS}^*) flattens or even slightly decreases with K (fig. 1*B*). In a negative feedback loop, increasing K elevates parasite density, selecting for more resistance and thereby lowering parasite density. Notably, the evolution of resistance enables hosts to attain increasing total host density (H_{CSS}^*; fig. 1*C*) and especially susceptible density ($S_{CSS}^* = m/(\sigma\beta_{CSS})$; fig. 1*D*) as K increases (relative to fixed β populations). Hence, this castration case conforms to typical predictions of the evolution of resistance: when ecological drivers create large epidemics, high resistance evolves, reducing prevalence and suppression of host density. We found oscillations only in the minority of parameter ranges ($\theta = 0$ and β_{medium} in $K = 86$–150 and β_{high} in $K = 16$–150); for all other parameter values reported here, we found only an approach to stable equilibria. In these cases, we averaged over the last third of a very long time series (days 6.67×10^4 to 10×10^4, otherwise following the simulation procedure described above) to estimate ecological outcomes. These averages qualitatively followed the same pattern as and form a continuous curve with stable equilibrium outcomes (see fig. 1*B*–1*D*).

When parasites allow reproduction (e.g., $\theta = 0.65$), qualitatively different eco-evolutionary dynamics and the resistance is futile effect emerge. As K increases, parasite density and prevalence once again increase. However, once these are sufficiently high ($p_{CSS}^* \approx 0.46$ and $K \approx 35$), the benefit of resistance declines and a resistance is futile scenario arises (fig. 1*E*). Instead of investing in increasing resistance, hosts invest in a faster foraging rate, despite a higher risk of infection. Notably, this switch occurs well before all individuals become infected. Now, positive feedbacks can arise between host evolution and parasite density; increased K elevates parasite density, selecting for less resistance, which further elevates parasite density. The stabilizing trade-off constrains these positive feedbacks, leading to high but biologically plausible β_{CSS}. However, positive feedbacks do create evolutionary bistability, where a repeller separates two CSSs (dashed curve: not convergence stable [nor evolutionarily stable]). Thus, at high enough K, resistance is not always "futile": hosts may evolve to high resistance (low β_{CSS}) if the population begins evolving at low enough β. Hence, unlike for the castration case, when infected hosts reproduce, the resistance is futile effect and bistability can both arise.

The resistance is futile mechanism has clear implications for prevalence and host density. At low K, evolution of increasing resistance slows (but does not prevent) an increase in prevalence (p_{CSS}^*; fig. 1*F*) with K. But at higher K, prevalence in the evolving host increases more quickly than for any ecological case (black square) unless hosts evolve to the resistant CSS (white triangle). That prevalence pattern approximates the response of the density of infected hosts (I^*) or parasite propagules (Z^*; both not shown). Increased prevalence strongly depresses host density; it can even decrease slightly with K (H_{CSS}^*; slight dip in black curve in fig. 1*G*; more dramatic for susceptible host density in fig. 1*H*). Hence, evolution toward the high-transmission-rate CSS results from selection on individual fitness and hurts the host population in terms of prevalence and host density.

The fecundity of infected hosts attracts host evolution toward a high-fecundity and low-resistance state, thereby

inflicting damage on host density. This result becomes very clear when comparing ecological host densities with and without castration to eco-evolutionary densities. All else equal and without evolution (ecology only), a castrating parasite hurts infected individuals more (i.e., is more "virulent") and more strongly suppresses host density (compare gray curves in fig. 1*C*–1*G*, especially the lower-resistance curves, which experience more infection and castration; Anderson and May 1981). But once hosts can evolve, less severe fecundity reduction (less virulence) on individuals ends up leading to stronger suppression of host density with the resistance is futile effect (black curves in fig. 1*C* vs. 1*G*), particularly for susceptible hosts (S^*, fig. 1*D* vs. 2*H*). Hence, because of eco-evolutionary dynamics, the less virulent parasite can suppress host density more than a more virulent one.

Further study of this model expands the scope of the resistance is futile result in three ways (supplemental PDF, sec. 1). First, it can arise at various carrying capacities (K) and prevalence levels (p). On the one hand, it may require higher K with more harmful parasites (lower θ or higher v; fig. S1*A*, S1*B*). Nonetheless, high K will still trigger a resistance is futile effect unless parasites eliminate the fitness of infected hosts (through complete castration, $\theta = 0$, or instant killing as with predation, $v = \infty$; fig. S1); without the fitness of infected hosts, a driver that acts through

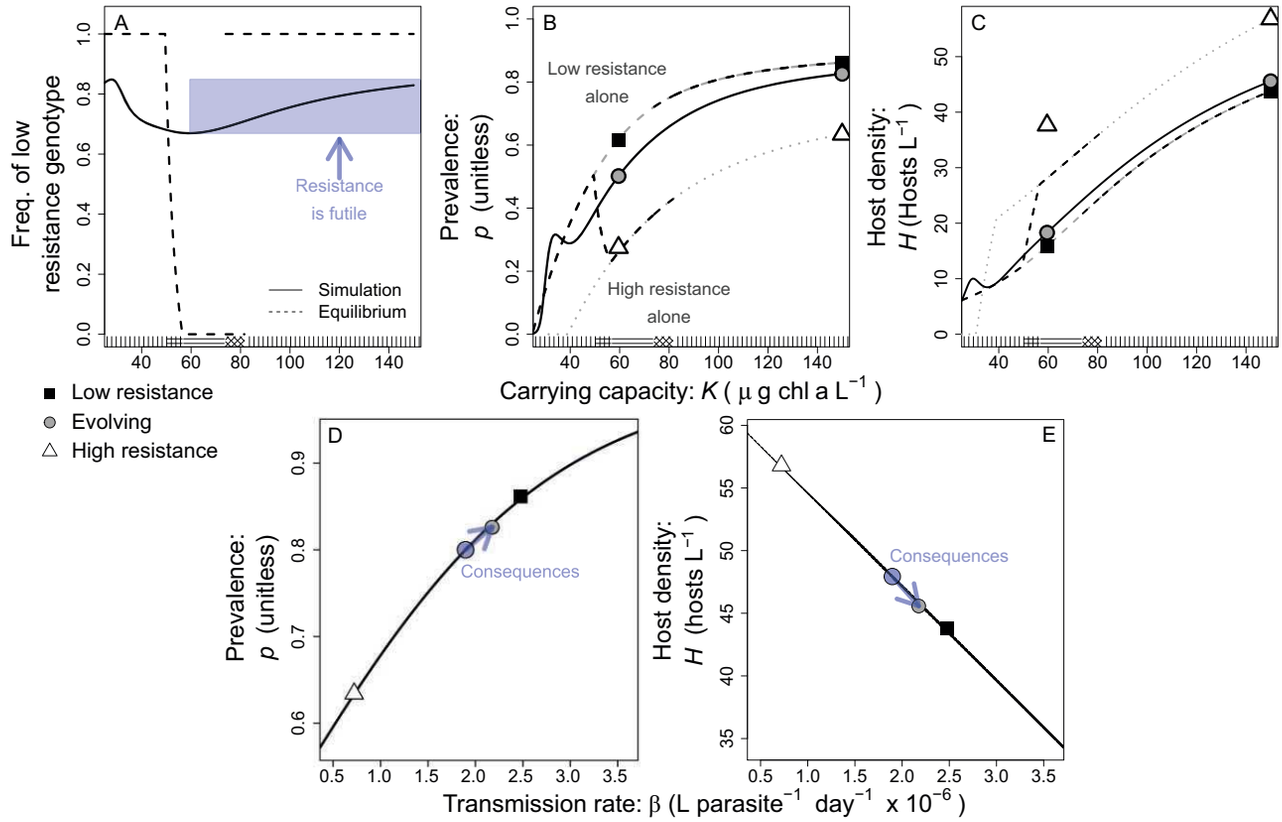

Figure 2: Increasing carrying capacity selects for higher, then lower, resistance. We show stable equilibria for each genotype (gray curves = low [dashed] and high [dotted] resistance) or the two-genotype system (dashed black). The solid black curve shows simulation outcomes (averaged from days 100 to 150, as described in the main text). The blue rectangle highlights the carrying capacity (K) where the resistance is futile effect arises for simulations. Symbols highlight simulation outcomes with low resistance (black squares), high resistance (white triangles), or both genotypes (gray circles) at low and high K values (to guide interpretation of the experiment; see the main text); because simulations have not reached equilibrium, symbols need not lie on any dashed curves (dashed curves show stable equilibria). *A*, Vertical hatching on the x-axis denotes fixation by the low-resistance genotype, while horizontal hatching denotes fixation by the high-resistance genotype; vertical-horizontal crosshatching denotes coexistence (lower K), and diagonal crosshatching denotes priority effects (higher K). The pattern is similar but without fixation in evolving simulations (solid black curve). *B*, K and transmission rate increase prevalence, p. *C*–*E*, K increases host density, H, and transmission rate decreases H (*C*). Then the simulation results forecast how the resistance is futile effect impacts prevalence (*D*) and host density (*E*) at high K (150). Regression lines connect prevalence/density to transmission rate. The blue circle shows hypothetical prevalence/density, and the gray circle shows actual prevalence/density. The blue arrow connecting them shows the consequence of the resistance is futile effect (as shown in fig. 3; see the main text for more explanation).

increased parasite density, Z^*, drives evolution toward more resistance (assuming that evolution is a continuous function of the driver, as we find in fig. 1*A*; for proof, see the supplemental PDF, sec. 1). On the other hand, it can also begin at a quite low prevalence (fig. S1*C*, S1*D*), depending on trait values. Second, resource feedbacks underlie the resistance is futile scenario. In particular, the trophic cascade created by parasites elevates resource density so that a higher birth rate can compensate for the higher mortality caused by the epidemic (fig. S4*A*). Third, the resistance is futile effect arises along gradients of other ecological drivers of parasite abundance. In these other cases, evolution of lower resistance increases prevalence and suppresses host density as well (figs. S5, S6). Overall, the resistance is futile effect can emerge in a variety of scenarios that may matter for diverse biological populations.

Results: Two-Genotype Model, Equilibrial and Nonequilibrial Dynamics

The same general patterns of the resistance is futile effect arise for the two-genotype model. At low K, there is little infection and the low-resistant genotype fixes (vertical hatching in fig. 2*A*). As K increases, infection increases and the system transitions to coexistence of the genotypes (cross-hatching), then the high-resistance genotype fixes (horizontal hatching). However, as K increases still further, the resistance is futile effect becomes possible. As prevalence in each genotype rises (fig. S4*B*), the difference in prevalence—and the benefit of resistance—is maximized at intermediate K (fig. S4*C*). Hence, at high K the benefit of resistance is small. There, selection favors high foraging rate/transmission rate, leading to a higher prevalence and release of more parasite propagules. This positive feedback loop leads to alternative stable states (i.e., priority effects) between fixation of the two genotypes (solid black). When the high-resistance genotype fixes, parasite propagules are less abundant and resistance is worthwhile. When the low-resistance genotype fixes, parasite propagules are more abundant and resistance becomes futile. At even higher K, parasite propagules become abundant enough that resistance is futile regardless of initial conditions. There, the low-resistance genotype always fixes. This clonal competition is qualitatively similar to results from continuous trait evolution (fig. 1*E*) and leads to similar results for prevalence (compare fig. 1*F* with 2*B*) and host density (compare fig. 1*G* with 2*C*).

Simulations of the two-genotype evolution qualitatively follow the trend of stable equilibria. Throughout our K range and for each genotype alone or both together, we analytically find that one or two stable equilibria and simulations approach these; in all of these cases, our simulations asymptotically approached these equilibria, failing to find any exotic features, such as stable limit cycles. These simulations provide a qualitative comparison to trends in the mesocosm experiment (described in the next section). Simulations with both genotypes started with equal frequencies. For reference to the experiment, we also simulated ecology-only outcomes with only the low-resistance genotype (black squares) or the high-resistance genotype (white triangles).

We use the simulation results to illustrate the impact of the resistance is futile effect on prevalence and host density in the experiment. The approach involves a quantitative thought exercise. In both the simulation (here; fig. 2) and the experiment (below; fig. 3), hosts evolved lower resistance (higher β) in the high-carrying-capacity treatment ($K = 150$ vs. $K = 63$ in the simulations). To estimate the consequences of such evolution, we imagine that the host instead evolved to the higher resistance (lower β) achieved in the lower-K treatment (likely a conservative value). Then, given that higher resistance level, we estimate what prevalence of infection (p) and host density (H) could have been reached. However, this inference requires care, as the β-p and β-H relationships differ between low and high K. Hence, we first fitted a beta regression to estimate the β-p relationship at high K and a linear one to estimate the β-K relationship. We then used those regressions to calculate what hypothetical prevalence and density would have been reached (given higher resistance; blue circle) versus what was reached (in reality; gray circle; figs. 2*D*, 2*E*, 3*D*, 3*E*). The consequences of the resistance is futile effect then follow: the arrows point to the increase in prevalence and decline in host density caused by this evolutionary response.

Eco-Evolutionary Outcomes from Selection on Resistance: Experiment

Methods

We tested predictions of the model by creating experimental epidemics with a plankton system. This system meets many assumptions of the model. The host, the zooplankton grazer *Daphnia dentifera*, feeds on an alga, *Ankistrodesmus falcatus*. The carrying capacity of this resource depends on nutrient supply. Then, because hosts ingest infectious spores, they trade off the foraging rate (and hence the birth rate) with the transmission rate of a fungal parasite, *Metschnikowia bicuspidata* (Hall et al. 2010, 2012; Auld et al. 2013). Hosts also vary in susceptibility to terminal infection once exposed (Stewart Merrill et al. 2019; Strauss et al. 2019); this variation forms part of the trade-off. Infected hosts retain significant fecundity, providing a test for the noncastration

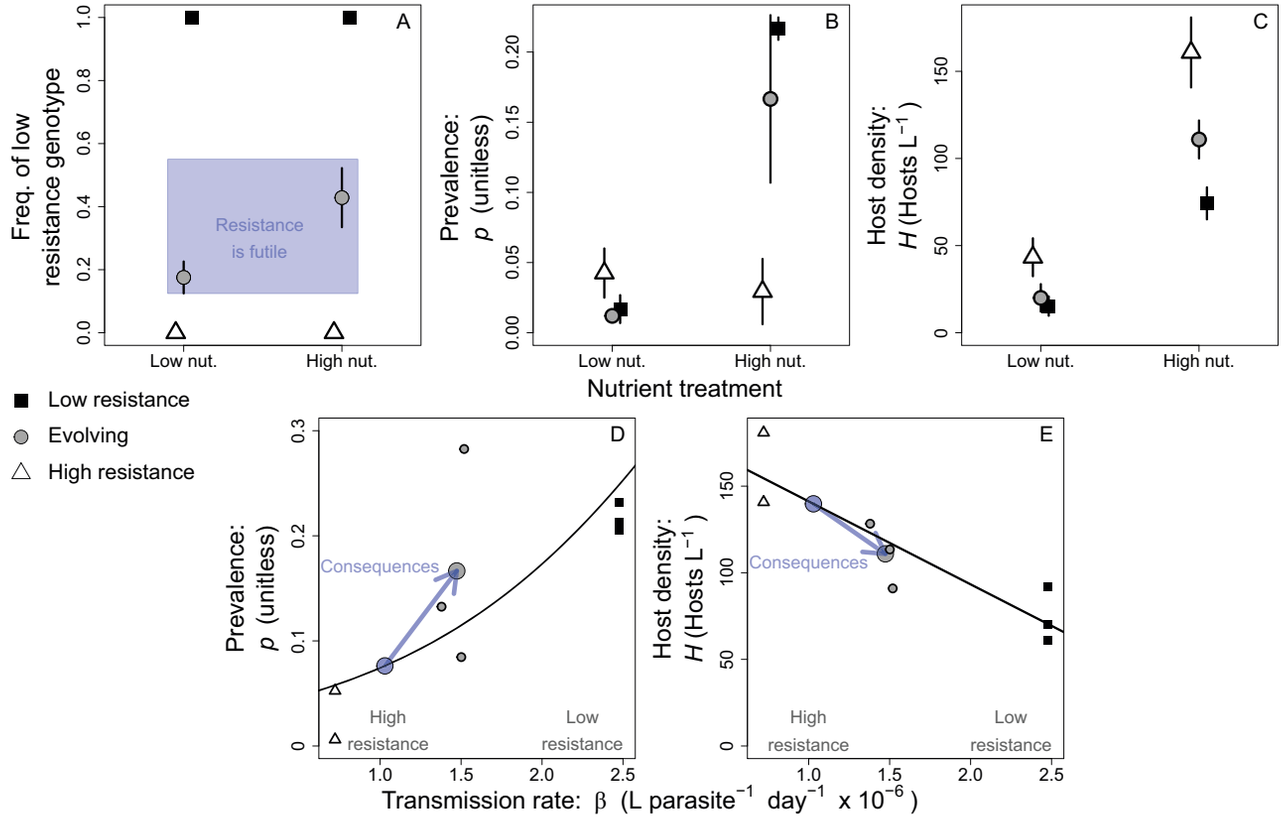

Figure 3: Implications of an epidemic driver (nutrient supply) for resistance, prevalence, and host density in populations that can evolve, relative to ecology-only controls. Symbols denote genotype treatments with approximately three replicates each (see the main text). *A*, Resistance: high-nutrient populations were less resistant than low-nutrient populations, consistent with a resistance is futile effect (see *K* increasing frequency of less resistant genotype in fig. 2*A*). Bars show ±1 SE calculated over two time points and replicates within a treatment. *B*, Prevalence (p) averaged over time and treatment for low-resistance (squares), high-resistance (triangles), and evolving-resistance (circles) genotype treatments. High-resistance populations have lower prevalence. Higher nutrients increase p, but not for high-resistance populations (similar to fig. 2*B*). *C*, High-resistance populations have higher host density (H). Higher nutrients increase H, especially for high-resistance populations (as in fig. 2*C*). *D*, *E*, At high nutrients, less resistance in *A* was significantly associated with higher p (*D*) and lower H (*E*). Blue points represent hypothetical prevalence and host density (as in fig. 2*D*, 2*E*), and large gray points show actual treatment means. Blue arrows connect these points, illustrating the consequences of the resistance is futile effect for prevalence and host density.

case (Hall et al. 2010). In the 50-L mesocosms, thousands of individuals interacted dynamically with resources and parasites (as in the model) for approximately 10 host generations.

We stocked mesocosms with two clonal genotypes of hosts with known (premeasured) traits (Strauss et al. 2015; Walsman et al. 2022*b*). In monoclonal, "ecology-only" reference mesocosms, we added either a genotype with high resistance but slower foraging (hereafter, "high-resistance genotype") or one with lower resistance but a higher foraging rate (hereafter, "low-resistance genotype"; mimicking the gray nonevolving curves in fig. 1). In "evolving" mesocosms, we introduced both genotypes at equal frequency, and then clonal frequency changed as they competed during epidemics. These three host treatments were crossed with two nutrient levels (to mimic low and high K), yielding a 3 × 2 design with three replicates. Of these 18 populations, two outliers were excluded in the final analysis (for more details, see the supplemental PDF, sec. 2). We sampled hosts twice a week to estimate density and prevalence. We used these samples of hosts twice during the epidemic to genotype each evolving population (see the supplemental PDF, sec. 2).

This experiment tested qualitative predictions of our model. Specifically, compared with populations that received a lower supply of nutrients, those with a high nutrient supply may experience the resistance is futile effect, leading to larger epidemics, lower resistance, and lower host density. We tested whether nutrients increased prevalence and host density with a beta regression (because

prevalence is bounded between 0 and 1), and we used a linear model for host density (see the supplemental PDF, sec. 2). We calculated the mean transmission rate (β) for evolving populations as the frequency-weighted average of clonal estimates of that trait (collected 16 and 24 days after spore addition; see the supplemental PDF, sec. 2). We tested whether genotype frequency differed between nutrient supply treatments using a logistic regression of genotype identity on nutrients with mesocosm as a random effect. We then evaluated the relationship between the transmission rate (x-axis) and prevalence (y-axis, beta regression) or host density (y-axis, total and infected, linear model) at each nutrient level (for details, see the supplemental PDF, sec. 2). The ecological results here (host density and prevalence) were reported previously as part of a larger experiment, with a different focus and analysis (Walsman et al. 2022*b*). In contrast, the evolutionary results (host genotype frequencies and calculated average transmission rate) are reported here for the first time.

Results

The experimental results qualitatively matched the eco-evolutionary model phenomenon of resistance being futile: lower resistance evolved when epidemic drivers were high compared with when they were low. In evolving populations, the frequency of the low-resistance genotype increased from 17.5% at low nutrient supply to 42.9% at high nutrient supply ($P = .0415$ with 85 individuals genotyped; fig. 3*A*). Nutrients increased prevalence ($P = .004$; fig. 3*B*) and host density ($P < .001$; fig. 3*C*).

The eco-evolutionary model predicts that a higher transmission rate should increase prevalence and infected host density while decreasing total host density. We used the single-genotype reference populations to determine the ecological effects of the transmission rate. At high nutrient supply, a higher transmission rate was associated with higher prevalence ($P = .002$; beta regression curve in fig. 3*D*) and lower host density ($P = .002$; line in fig. 3*E*); infected host density had a nonsignificant positive association ($P = .226$; not shown). These regressions allowed us to evaluate the impact of the resistance is futile effect using the quantitative thought exercise described above. More specifically, the regression enabled estimation of hypothetical prevalence (blue point in fig. 3*D*) and host density (blue point in fig. 3*E*) if hosts had evolved as much resistance at high nutrient supply as at low supply (as in fig. 2*D*, 2*E*). The arrows, then, connect these hypothetical values to those reached in the actual mesocosms (large gray points). These arrows point out how the resistance is futile mechanism amplified prevalence (fig. 3*D*) and suppressed host density (fig. 3*E*), as predicted (see fig. 2*D*, 2*E*, respectively).

Comparison of the Distributions of Epidemic Size: Models and the Field

Methods

If the resistance is futile effect can occur in mesocosms, does it matter in nature? While this would be difficult to test directly, we examined whether preliminary evidence is consistent with the resistance is futile prediction. As we will show below, the positive feedbacks of the resistance is futile effect should make the distribution of epidemic size broader, somewhat bimodal, and right skewed. We tested this prediction using the distribution of natural fungal epidemics. We sampled epidemics in Indiana lakes during the period 2009–2016 (166 unique lake-years) and measured the prevalence of fungal infection multiple times over the epidemic season (for details, see the supplemental PDF, sec. 3). We consider epidemic size in a given lake-year as the maximum prevalence attained over the epidemic season (correlated with mean prevalence; fig. S7). We consider only lakes that had an epidemic (defined as reaching a maximum prevalence of ≥ 0.1; table S1 shows how these results shift somewhat if we use mean or maximum prevalence and alter threshold choice). We compare this field distribution (fig. 4*A*) to those produced from the eco-evolutionary model, given a distribution of the carrying capacity of the resource. (We chose K as the focal ecological driver because it influenced prevalence in the model and experiment, and likely in the field as well; see fig. S7).

Model distributions were generated under two cases of host evolution in the model with some fecundity while infected ($\theta = 0.65$). Normal distributions of K in the model had their mean and standard deviation fitted to maximize their match to the field data for each model case (for details, see the supplemental PDF, sec. 3). In the "constrained" case, we force hosts to evolve more resistance with K. To implement this constraint, we use trait values across K from the castration case, in which hosts only evolve increasing resistance with K (fig. 1*A*). The different implementation method of this case did not qualitatively affect the outcomes (not shown). In the resistance is futile case, hosts evolve normally; hence, resistance can increase and then decrease with K (as in fig. 1*E*; see fig. 4*B*). Because of unmeasured factors in natural populations (e.g., various other ecological drivers), we did not expect a precise match between distributions of prevalence in the model and field. Instead, we measured the deviations between them with descriptive statistics of breadth and shape: the interquartile range (IQR), bimodality (Ashman's D [AshD]), and right skew. A lower sum of relative deviations provided a better fit (found for each case using a genetic algorithm; see the supplemental PDF, sec. 3).

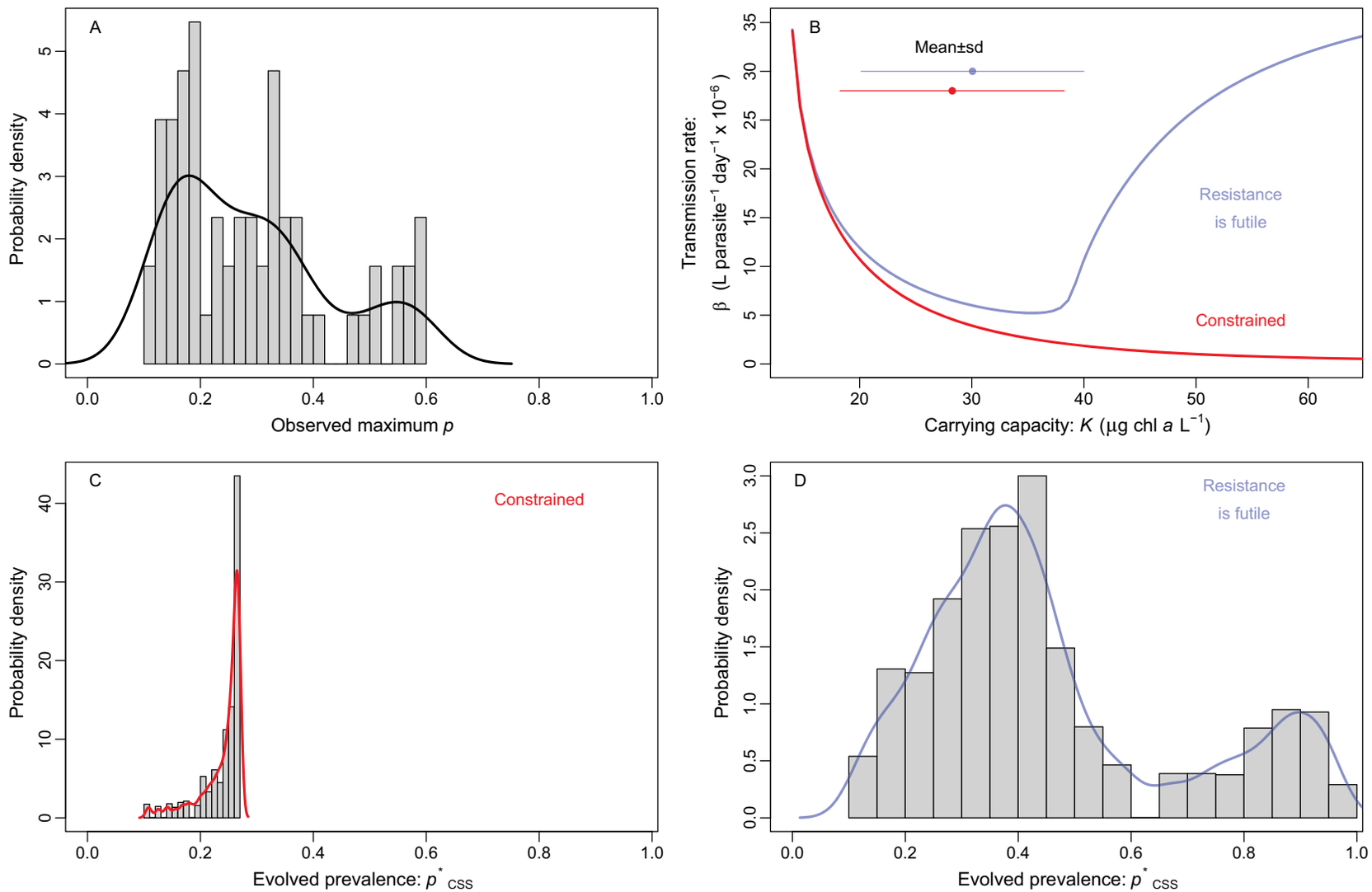

Figure 4: Comparison of model predictions and natural prevalence. *A*, Maximum prevalence in epidemics of the virulent fungus in Indiana lakes. Curves on histograms are smooth probability densities. *B*, In the two model cases, hosts can evolve according to the resistance is futile effect (blue curve; compare with fig. 1*E*) or are constrained to only evolve increasing resistance with *K* (red curve). For each evolution case, we found the distribution of *K* yielding the best-fit distribution of prevalence. Solid points and bars at the top of the plot indicate the mean ± SD of (highly overlapping) best-fit *K* distributions for each model case. *C*, The constrained eco-evolutionary case produced a narrow distribution of prevalence that poorly matched the field data. *D*, The resistance is futile mechanism produced a broader, somewhat bimodal, right-skewed best-fit distribution that better fit prevalence in Indiana lakes (compare with *A*).

Results

Natural populations displayed a broad, somewhat bimodal, right-skewed distribution of prevalence. The observed distribution had an IQR of 0.184, an AshD of 2.123, and a skew of 0.716 (fig. 4*A*). Without the resistance is futile effect (i.e., following the constrained K-β relationship; fig. 4*B*), host evolution created a narrow (IQR = 0.049; fig. 4*C*), less bimodal (AshD = 1.790), and left-skewed (skew = −1.464) distribution with a poorer match to field data (summed relative deviance = 3.934). In contrast, the resistance is futile mechanism produced a broader distribution (IQR = 0.213; fig. 4*D*) with more bimodality and right skew (AshD = 4.576, skew = 0.920). Interestingly, the model did not fit high enough K values to fall in the range of bistability (for the 2,000 K values generated, see fig. 4*B* for mean and standard deviation) but generated bimodality simply from the shape of the β-K curve. These metrics better matched the field data (summed relative deviance = 1.602). The resistance is futile case produced larger IQR, AshD, and right skew because of positive feedbacks between parasite density and host evolution. Hence, the broad, bimodal, right-skewed distribution observed in nature is more consistent with predictions of positive feedbacks that arise only in the resistance is futile case of the eco-evolutionary model.

Discussion

One might expect hosts to evolve more resistance when ecological drivers favor high parasite abundance. However, we argue that those conditions can make resistance futile: more parasites can select for less resistance, which increases infection prevalence and depresses host density. We show this possibility in an eco-evolutionary model of a host-parasite-resource system using adaptive dynamics as well as equilibrial and transient competition between two clones. We confirm it qualitatively with a population-level experiment in a plankton system. Furthermore, the resistance is futile response can create positive feedbacks between host evolution and parasite density, which can even generate bistability (see two CSSs [fig. 1] and priority effects [fig. 2]). These positive feedbacks produced broad, somewhat bimodal, right-skewed distributions of prevalence in the model consistent with those observed in epidemics in lakes. Hence, our theory and experimental results, with support from the field survey, all suggest that resistance can become futile when ecological drivers lead to high parasite abundance.

Under what conditions do we expect to see the resistance is futile effect? First, hosts must pay a cost for resistance, for example, via a resistance-fecundity trade-off; otherwise, selection never decreases resistance. Second, the resistance is futile outcome would be less likely if resistance to infection also reduced the harm from infection; in the asymptotic case of 100% infection, the resistance is futile effect is driven by the fact that the lowest-resistance genotypes have the highest fitness when all genotypes are infected. Hence, we do not see the resistance is futile effect when parasites fully castrate (eliminate reproduction) or if hosts die immediately after infection (for proof, see the supplemental PDF, sec. 1; Leibold 1996; Bohannan and Lenski 1997, 2000; Lopez-Pascua et al. 2014). If hosts could plastically maximize their foraging rate once infected, this adaptive response would also undermine the resistance is futile effect, as all genotypes would have the same maximal foraging rate. Such a plastic maximization seems biologically unlikely in our focal system, as foraging rate decreases because of the burden of infection (Penczykowski et al. 2022). Third, ecological factors must favor high enough parasite abundance to render resistance futile. We demonstrate this idea (mathematically and empirically) using the carrying capacity of the resource (but also extend it to other growth and loss factors that influence parasite abundance).

How often do systems meet these conditions in nature? Various systems show the trade-off (Boots and Begon 1993; Kraaijeveld and Godfray 1997; Hall et al. 2010; Auld et al. 2013), hosts often/usually retain some fecundity while infected (Kuris et al. 2008), and many systems have a high prevalence of infection (Ezenwa 2004). Some systems may indeed meet all three requirements. For instance, a guppy-flatworm system likely possesses the trade-off (Huizinga et al. 2009; Hockley et al. 2014) while certainly retaining some fecundity while infected (Pérez-Jvostov et al. 2015) and reaching a high prevalence in nature (Stephenson et al. 2015). When these conditions are met, increased parasite abundance may undermine selection for resistance. However, we know of no other empirical demonstration—yet—of this phenomenon.

Our model builds on others that demonstrate when resistance is futile. Indeed, it arises in other models (Bonds et al. 2005; Miller et al. 2007; Donnelly et al. 2015; Best et al. 2017; Walsman and Cressler 2022), as does a similar form of evolutionary bistability (Miller et al. 2007; Best et al. 2017). All of these models, despite differences in details, share a common thread. In each, high enough parasite abundance and force of infection reduces the benefit of resistance. Instead, reproduction by infected hosts rewards lower resistance (due to the fecundity cost of resistance in a trade-off). Eventually, the cost of resistance outweighs the diminishing benefit of resistance. However, our work builds on previous work in two useful ways. First, we showed the implications of the resistance is futile effect for prevalence and host density with comparison to ecology-only populations. It may benefit more adaptive

dynamics analyses to make similar connections to ecological relevance, which is currently uncommon. Second, we show similar resistance is futile outcomes for resistance, prevalence, and density across three complementary modeling approaches. Harmony between the three modeling approaches ensured robustness of these findings while qualitatively simulating evolutionary outcomes in the experiment.

As importantly, we show direct experimental support for the resistance is futile effect. Specifically, the experiment saw hosts evolve less resistance during larger epidemics (created by higher nutrient supply) than during smaller epidemics. One other example (Parker 1991) showed evolution of decreased resistance during a large epidemic, but not along a gradient. In contrast, previous efforts showed evolution of higher resistance when ecological drivers lead to high parasite abundance (Duffy et al. 2012; Lopez-Pascua et al. 2014). Hence, the resistance is futile mechanism might explain why resistance and prevalence can correlate negatively in nature (Thrall and Burdon 2000; Laine 2004; Ericson and Burdon 2009). In a sense, the resistance is futile mechanism flips cause and effect: less resistance causes higher prevalence (a traditional explanation) or higher prevalence causes lower resistance through resistance is futile feedbacks (the new one here). The field survey of fungal epidemics in lakes was also consistent with a resistance is futile affect. Our model with resistance is futile–type evolution produced a broad, right-skewed, somewhat bimodal distribution of prevalence. That prediction better captured the qualitative shape of the field data than a resistance-only version of the model (a finding that, by itself, offers consistency but not conclusiveness). Hence, supported by the suggestive field pattern, the mesocosm data challenges expectations that conditions leading to higher parasite abundance should select for stronger resistance. They may not.

The implications of the resistance is futile effect for prevalence and host density raise broad ecological concerns. When hosts evolve high resistance, infection prevalence remains small, and parasites depress host density little (Altizer et al. 2003; Duffy and Sivars-Becker 2007; Christie and Searle 2018). If hosts instead evolve less resistance, parasites may depress host density more significantly. Furthermore, depressed density may threaten the persistence of host populations (Ebert et al. 2000; De Castro and Bolker 2005). Additionally, the resistance is futile effect can produce a high density of infected hosts (seen in the model, trended in the experiment). Higher infected density may increase the risk of spillover to other host species (Daszak et al. 2000; Power and Mitchell 2004). Hence, evolution of lower resistance may exacerbate the negative effects of ecological drivers of high parasite abundance for hosts of multiple species.

The resistance is futile effect resembles the evolution of tolerance in two ways, but they differ in one key aspect. First, evolution of lower resistance (higher fecundity) maximizes fitness of the infected host class. Similarly, tolerance minimizes virulence on fecundity (Restif and Koella 2004) or mortality (Boots and Bowers 1999; Miller et al. 2006). Hence, both strategies increase the fitness of infected hosts without eliminating infection. Second, both the resistance is futile effect and tolerance invoke positive feedbacks, where higher parasite density can select for less resistance or higher tolerance. Both responses lead to still higher parasite density (for tolerance, see Roy and Kirchner 2000; Miller et al. 2005, 2006). However, these mechanisms likely exert different consequences for host density. While lower resistance depresses host density, increased tolerance can elevate it (Miller et al. 2006). However, more complex possibilities arise: tolerance that lowers mortality may sometimes amplify directly transmitted disease, thereby suppressing host density (Anderson 1979). We suggest that reanalysis/future development of models of tolerance evolution (e.g., Boots et al. 2009; Cressler et al. 2015; Best et al. 2017) could clarify and contextualize how tolerance evolution impacts host density (as we did in figs. 1 and 2).

After establishing that the resistance is futile effect can arise, how do we know when and where to look for it in the future? First, to characterize the predicted U shape of the evolution of transmission rate, future tests of the eco-evolutionary model could employ a wider range and more levels of nutrient supply (fig. 1*E*). Second, to broaden and generalize, future tests should evaluate how other factors (besides nutrients) drive the resistance is futile effect (as we modeled). Factors that increase production of resources, hosts, and parasites and those that decrease losses of hosts and parasites could all trigger it. Third, to test for the predicted priority effects at higher nutrient supply, experiments could be started at different frequencies of genotypes (i.e., some starting at high resistance and others at low resistance). Fourth, to more conclusively evaluate predictions in the field, traits can be measured before and after epidemics (as in Duffy et al. 2012) during the largest epidemics (although this task can prove quite laborious). In addition, future theoretical work could alter key assumptions made here. First, other trait relationships can be included. For instance, if lower resistance increases mortality virulence (Hall et al. 2010), fitness advantages of low-resistance strategies would shrink. Second, parasite coevolution—say along a virulence-transmission tradeoff (Best et al. 2009)—could interact with these dynamics; for example, fast enough parasite evolution can stabilize positive feedbacks in the resistance is futile mechanism (see the supplemental material of Walsman and Cressler 2022). These extensions would highlight how and when

drivers of high parasite abundance should and should not lead to the resistance is futile effect.

This study warns that the evolution of lower resistance during larger epidemics may elevate prevalence and depress host density. This resistance is futile outcome broadens the range of eco-evolutionary possibilities during epidemics. Even more importantly, resistance is futile effects may increase prevalence and lower host density more commonly than anticipated. This possibility raises important implications for controlling the spread of disease. Yet this eco-evolutionary mechanism requires several components (fecundity-resistance trade-offs, reproduction by infected hosts, and sufficiently large epidemics). At this point, it remains unclear how many systems meet these assumptions. Just when will maximization of the fitness of individual hosts amplify already-large epidemics, and when/why will it not? Guided by theory, we now know where to look.

Acknowledgments

J. Obergfell, P. Orlando, and M. Šljivar provided assistance with the experiments. I. Menel assisted with genotyping at the Roy J. Carver Biotechnology Center at the University of Illinois at Urbana-Champaign. C. Lively, F. Bashey-Visser, M. Wade, A. Ramesh, and T. Deblieux provided valuable feedback on the manuscript. This work was supported by National Science Foundation grants DEB 1353749, DEB 1655656, and GRFP 1342962 to J.C.W.

Statement of Authorship

All authors contributed to conceptualization and funding acquisition. J.C.W., C.E.C., and S.R.H. contributed to methods development. J.C.W. and S.R.H. contributed to the experimental design. J.C.W. conducted data collection, data analysis, data validation, and data visualization. C.E.C. and S.R.H. provided resources. J.C.W. preformed the theoretical modeling. J.C.W. and S.R.H. wrote the original draft. All authors contributed to reviewing and editing the manuscript.

Data and Code Availability

All data and code are available in the Dryad Digital Repository (https://doi.org/10.5061/dryad.q573n5tn5; Walsman et al. 2022*a*).

Literature Cited

Altizer, S., D. Harvell, and E. Friedle. 2003. Rapid evolutionary dynamics and disease threats to biodiversity. Trends in Ecology and Evolution 18:589–596.

Anderson, R. M. 1979. Parasite pathogenicity and the depression of host population equilibria. Nature 279:150–152.

Anderson, R. M., and R. M. May. 1981. The population dynamics of microparasites and their invertebrate hosts. Philosophical Transactions of the Royal Society B 291:451–524.

Auld, S. K. J. R., R. M. Penczykowski, J. H. Ochs, D. C. Grippi, S. R. Hall, and M. A. Duffy. 2013. Variation in costs of parasite resistance among natural host populations. Journal of Evolutionary Biology 26:2479–2486.

Best, A., A. White, and M. Boots. 2009. The implications of coevolutionary dynamics to host-parasite interactions. American Naturalist 173:779–791.

———. 2017. The evolution of host defence when parasites impact reproduction. Evolutionary Ecology Research 18:393–409.

Bohannan, B. J. M., and R. E. Lenski. 1997. Effect of resource enrichment on a chemostat community of bacteria and bacteriophage. Ecology 78:2303–2315.

———. 2000. The relative importance of competition and predation varies with productivity in a model community. American Naturalist 156:329–340.

Bonds, M. H., D. C. Keenan, A. J. Leidner, and P. Rohani. 2005. Higher disease prevalence can induce greater sociality: a game theoretic coevolutionary model. Evolution 59:1859–1866.

Boots, M., and M. Begon. 1993. Trade-offs with resistance to a granulosis-virus in the Indian meal moth, examined by a laboratory evolution experiment. Functional Ecology 7:528–534.

Boots, M., A. Best, M. R. Miller, and A. White. 2009. The role of ecological feedbacks in the evolution of host defence: what does theory tell us? Philosophical Transactions of the Royal Society B 364:27–36.

Boots, M., and R. G. Bowers. 1999. Three mechanisms of host resistance to microparasites—avoidance, recovery and tolerance—show different evolutionary dynamics. Journal of Theoretical Biology 201:13–23.

Boots, M., and Y. Haraguchi. 1999. The evolution of costly resistance in host-parasite systems. American Naturalist 153:359–370.

Carlson, S. M., C. J. Cunningham, and P. A. Westley. 2014. Evolutionary rescue in a changing world. Trends in Ecology and Evolution 29:521–530.

Christie, M. R., and C. L. Searle. 2018. Evolutionary rescue in a host-pathogen system results in coexistence not clearance. Evolutionary Applications 11:681–693.

Cooper, J., R. J. Crawford, M. S. De Villiers, B. M. Dyer, G. G. Hofmeyr, and A. Jonker. 2009. Disease outbreaks among penguins at sub-Antarctic Marion Island: a conservation concern. Marine Ornithology 37:193–196.

Cressler, C. E., A. L. Graham, and T. Day. 2015. Evolution of hosts paying manifold costs of defence. Proceedings of the Royal Society B 282:20150065.

Daszak, P., A. A. Cunningham, and A. D. Hyatt. 2000. Emerging infectious diseases of wildlife—threats to biodiversity and human health. Science 287:443–449.

De Castro, F., and B. Bolker. 2005. Mechanisms of disease-induced extinction. Ecology Letters 8:117–126.

Dobson, A., K. D. Lafferty, A. M. Kuris, R. F. Hechinger, and W. Jetz. 2008. Homage to Linnaeus: how many parasites? how many hosts? Proceedings of the National Academy of Sciences of the USA 105:11482–11489.

Donnelly, R., A. White, and M. Boots. 2015. The epidemiological feedbacks critical to the evolution of host immunity. Journal of Evolutionary Biology 28:2042–2053.

Duffy, M. A., and S. E. Forde. 2009. Ecological feedbacks and the evolution of resistance. Journal of Animal Ecology 78:1106–1112.

Duffy, M. A., S. R. Hall, C. E. Cáceres, and A. R. Ives. 2009. Rapid evolution, seasonality, and the termination of parasite epidemics. Ecology 90:1441–1448.

Duffy, M. A., J. H. Ochs, R. M. Penczykowski, D. J. Civitello, C. A. Klausmeier, and S. R. Hall. 2012. Ecological context influences epidemic size and parasite-driven evolution. Science 335:1636–1638.

Duffy, M. A., and L. Sivars-Becker. 2007. Rapid evolution and ecological host-parasite dynamics. Ecology Letters 10:44–53.

Duncan, A. B., S. Fellous, and O. Kaltz. 2011. Reverse evolution: selection against costly resistance in disease-free microcosm populations of *Paramecium caudatum*. Evolution 65:3462–3474.

Ebert, D., M. Lipsitch, and K. L. Mangin. 2000. The effect of parasites on host population density and extinction: experimental epidemiology with *Daphnia* and six microparasites. American Naturalist 156:459–477.

Ericson, L., and J. J. Burdon. 2009. Linking field epidemiological and individual plant resistance patterns in the *Betula pubescens-Melampsoridium betulinum* host-pathogen interaction. Oikos 118:225–232.

Eshel, I. 1983. Evolutionary and continuous stability. Journal of Theoretical Biology 103:99–111.

Ezenwa, V. O. 2004. Host social behavior and parasitic infection: a multifactorial approach. Behavioral Ecology 15:446–454.

Frank, S. A. 1994. Coevolutionary genetics of hosts and parasites with quantitative inheritance. Evolutionary Ecology 8:74–94.

Gomez, P., J. Bennie, K. J. Gaston, and A. Buckling. 2015. The impact of resource availability on bacterial resistance to phages in soil. PLoS ONE 10:e0123752.

Hall, S. R., C. R. Becker, M. A. Duffy, and C. E. Cáceres. 2010. Variation in resource acquisition and use among host clones creates key epidemiological trade-offs. American Naturalist 176:557–565.

———. 2012. A power–efficiency trade-off in resource use alters epidemiological relationships. Ecology 93:645–656.

Hockley, F. A., C. Wilson, N. Graham, and J. Cable. 2014. Combined effects of flow condition and parasitism on shoaling behaviour of female guppies *Poecilia reticulata*. Behavioral Ecology and Sociobiology 68:1513–1520.

Horan, R. D., and E. P. Fenichel. 2007. Economics and ecology of managing emerging infectious animal diseases. American Journal of Agricultural Economics 89:1232–1238.

Huizinga, M., C. Ghalambor, and D. Reznick. 2009. The genetic and environmental basis of adaptive differences in shoaling behaviour among populations of Trinidadian guppies, *Poecilia reticulata*. Journal of Evolutionary Biology 22:1860–1866.

Hurford, A., D. Cownden, and T. Day. 2009. Next-generation tools for evolutionary invasion analyses. Journal of the Royal Society Interface 7:561–571.

Koskella, B. 2018. Resistance gained, resistance lost: an explanation for host–parasite coexistence. PLoS Biology 16:e3000013.

Kraaijeveld, A. R., and H. C. J. Godfray. 1997. Trade-off between parasitoid resistance and larval competitive ability in *Drosophila melanogaster*. Nature 389:278–280.

Kuris, A. M., R. F. Hechinger, J. C. Shaw, K. L. Whitney, L. Aguirre-Macedo, C. A. Boch, A. P. Dobson, et al. 2008. Ecosystem energetic implications of parasite and free-living biomass in three estuaries. Nature 454:515–518.

Laine, A. L. 2004. Resistance variation within and among host populations in a plant–pathogen metapopulation: implications for regional pathogen dynamics. Journal of Ecology 92:990–1000.

Leibold, M. A. 1996. A graphical model of keystone predators in food webs: trophic regulation of abundance, incidence, and diversity patterns in communities. American Naturalist 147:784–812.

Lopez-Pascua, L. D., A. R. Hall, A. Best, A. D. Morgan, M. Boots, and A. Buckling. 2014. Higher resources decrease fluctuating selection during host-parasite coevolution. Ecology Letters 17:1380–1388.

Miller, M. R., A. White, and M. Boots. 2005. The evolution of host resistance: tolerance and control as distinct strategies. Journal of Theoretical Biology 236:198–207.

———. 2006. The evolution of parasites in response to tolerance in their hosts: the good, the bad, and apparent commensalism. Evolution 60:945–956.

———. 2007. Host life span and the evolution of resistance characteristics. Evolution 61:2–14.

O'Hara, N. B., J. S. Rest, and S. J. Franks. 2016. Increased susceptibility to fungal disease accompanies adaptation to drought in *Brassica rapa*. Evolution 70:241–248.

Parker, M. A. 1991. Nonadaptive evolution of disease resistance in an annual legume. Evolution 45:1209–1217.

Penczykowski, R. M., S. E. Forde, and M. A. Duffy. 2011. Rapid evolution as a possible constraint on emerging infectious diseases. Freshwater Biology 56:689–704.

Penczykowski, R. M., M. S. Shocket, J. H. Ochs, B. C. Lemanski, H. Sundar, M. A. Duffy, and S. R. Hall. 2022. Virulent disease epidemics can increase host density by depressing foraging of hosts. American Naturalist 199:75–90.

Pérez-Jvostov, F., A. P. Hendry, G. F. Fussmann, and M. E. Scott. 2015. Testing for local host–parasite adaptation: an experiment with *Gyrodactylus* ectoparasites and guppy hosts. International Journal for Parasitology 45:409–417.

Power, A. G., and C. E. Mitchell. 2004. Pathogen spillover in disease epidemics. American Naturalist 164:S79–S89.

Rankin, D. J., and A. López-Sepulcre. 2005. Can adaptation lead to extinction? Oikos 111:616–619.

Restif, O., and J. C. Koella. 2004. Concurrent evolution of resistance and tolerance to pathogens. American Naturalist 164:E90–E102.

Roy, B., and J. Kirchner. 2000. Evolutionary dynamics of pathogen resistance and tolerance. Evolution 54:51–63.

Slowinski, S. P., L. T. Morran, R. C. Parrish, E. R. Cui, A. Bhattacharya, C. M. Lively, and P. C. Phillips. 2016. Coevolutionary interactions with parasites constrain the spread of self-fertilization into outcrossing host populations. Evolution 70:2632–2639.

Soetaert, K., T. Petzoldt, and R. W. Setzer. 2010. deSolve: solving differential equations in R. Journal of Statistical Software 33:1–25.

Stephenson, J. F., C. Van Oosterhout, R. S. Mohammed, and J. Cable. 2015. Parasites of Trinidadian guppies: evidence for sex- and age-specific trait-mediated indirect effects of predators. Ecology 96:489–498.

Stewart Merrill, T. E., S. R. Hall, L. Merrill, and C. E. Cáceres. 2019. Variation in immune defense shapes disease outcomes in laboratory and wild *Daphnia*. Integrative and Comparative Biology 59:1203–1219.

Strauss, A. T., D. J. Civitello, C. E. Cáceres, and S. R. Hall. 2015. Success, failure and ambiguity of the dilution effect among competitors. Ecology Letters 18:916–926.

Strauss, A. T., J. L. Hite, D. J. Civitello, M. S. Shocket, C. E. Cáceres, and S. R. Hall. 2019. Genotypic variation in parasite avoidance behaviour and other mechanistic, nonlinear components of transmission. Proceedings of the Royal Society B 286:20192164.

Thrall, P., and J. Burdon. 2000. Effect of resistance variation in a natural plant host–pathogen metapopulation on disease dynamics. Plant Pathology 49:767–773.

van der Most, P. J., B. de Jong, H. K. Parmentier, and S. Verhulst. 2011. Trade-off between growth and immune function: a meta-analysis of selection experiments. Functional Ecology 25:74–80.

Vredenburg, V. T., R. A. Knapp, T. S. Tunstall, and C. J. Briggs. 2010. Dynamics of an emerging disease drive large-scale amphibian population extinctions. Proceedings of the National Academy of Sciences of the USA 107:9689–9694.

Walsman, J. C., and C. E. Cressler. 2022. Predation shifts coevolution toward higher host contact rate and parasite virulence. Proceedings of the Royal Society B 289:20212800.

Walsman, J. C., M. A. Duffy, C. E. Cáceres, and S. R. Hall. 2022*a*. Data and code from: "Resistance is futile": weaker selection for resistance by abundant parasites increases prevalence and depresses host density. American Naturalist, Dryad Digital Repository, https://doi.org/10.5061/dryad.q573n5tn5.

Walsman, J. C., A. T. Strauss, and S. R. Hall. 2022*b*. Parasite-driven cascades or hydra effects: susceptibility and foraging depression shape parasite–host–resource interactions. Functional Ecology 36:1268–1278.

References Cited Only in the Online Enhancements

Ashman, K. M., C. M. Bird, and S. E. Zepf. 1994. Detecting bimodality in astronomical datasets. Astronomical Journal 108:2348–2361.

Brännström, Å., J. Johansson, and N. von Festenberg. 2013. The hitchhiker's guide to adaptive dynamics. Games 4:304.

Ferrari, S., and F. Cribari-Neto. 2004. Beta regression for modelling rates and proportions. Journal of Applied Statistics 31:799–815.

Mangiafico, S. S. 2016. Summary and analysis of extension program evaluation in R. Version 1.18.1.

Prepas, E., and F. Rigler. 1982. Improvements in quantifying the phosphorus concentration in lake water. Canadian Journal of Fisheries and Aquatic Sciences 39:822–829.

R Core Team. 2019. R: a language and environment for statistical computing. R Foundation for Statistical Computing, Vienna.

Shi, S., D. Guo, and J. Luo. 2017. Enhanced phase and amplitude image contrasts of polymers in bimodal atomic force microscopy. RSC Advances 7:11768–11776.

Shocket, M. S., D. Vergara, A. J. Sickbert, J. M. Walsman, A. T. Strauss, J. L. Hite, M. A. Duffy, et al. 2018. Parasite rearing and infection temperatures jointly influence disease transmission and shape seasonality of epidemics. Ecology 99:1975–1987.

Strauss, A. T., J. L. Hite, M. S. Shocket, C. E. Cáceres, M. A. Duffy, and S. R. Hall. 2017. Rapid evolution rescues hosts from competition and disease but—despite a dilution effect—increases the density of infected hosts. Proceedings of the Royal Society B 284:20171970.

Whitley, D. 1994. A genetic algorithm tutorial. Statistics and Computing 4:65–85.

Associate Editor: Éva Kisdi
Editor: Erol Akçay

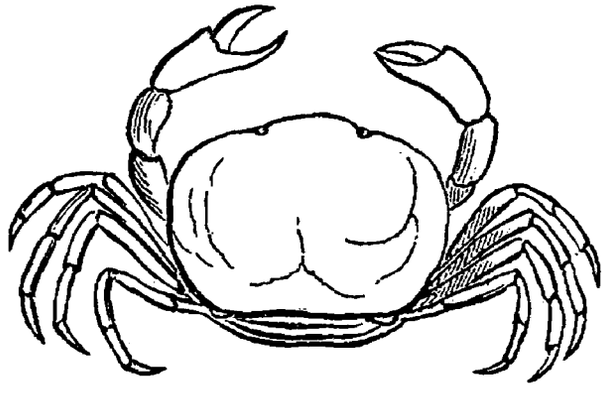

"Most persons have no doubt seen the little crab, with a smooth, rounded body, that lives in the interior of the shell between the gills of the oyster, and is often cooked with that excellent bivalve. This is the *Pinnotheres ostreum* [figured], and is doubtless parasitic in the oyster merely for the sake of shelter, and probably does not injure the oyster unless by the irritation that its motions might cause." From "On the Parasitic Habits of Crustacea" by A. E. Verrill (*The American Naturalist*, 1869, 3:239–250).